



Since January 2020 Elsevier has created a COVID-19 resource centre with free information in English and Mandarin on the novel coronavirus COVID-19. The COVID-19 resource centre is hosted on Elsevier Connect, the company's public news and information website.

Elsevier hereby grants permission to make all its COVID-19-related research that is available on the COVID-19 resource centre - including this research content - immediately available in PubMed Central and other publicly funded repositories, such as the WHO COVID database with rights for unrestricted research re-use and analyses in any form or by any means with acknowledgement of the original source. These permissions are granted for free by Elsevier for as long as the COVID-19 resource centre remains active.

# Identification of a Specific Interaction between the Coronavirus Mouse Hepatitis Virus A59 Nucleocapsid Protein and Packaging Signal

Richard Molenkamp and Willy J. M. Spaan<sup>1</sup>

Department of Virology, Institute of Medical Microbiology, Leiden University, AZL-L4-Q, P.O. Box 9600, 2300 RC Leiden, the Netherlands

Received July 21, 1997; returned to author for revision August 20, 1997; accepted September 25, 1997

The coronavirus mouse hepatitis virus (MHV) is an enveloped positive stranded RNA virus. In infected cells MHV produces a 3' coterminal nested set of subgenomic messenger RNAs. Only the genomic RNA, however, is encapsidated by the nucleocapsid protein and incorporated in infectious MHV virions. It is believed that an RNA packaging signal (Ps), present only in the genomic RNA, is responsible for this selectivity. Earlier studies mapped this signal to a 69-nt stem-loop structure positioned in the 3' end of ORF1b. The selective encapsidation mechanism probably initiates by specific interaction of the packaging signal with the nucleocapsid protein. In this study we demonstrate the *in vitro* interaction of the MHV-A59 nucleocapsid protein with the packaging signal of MHV using gel retardation and UV cross-linking assays. This interaction was observed not only with the nucleocapsid protein from infected cells but also with that from purified virions and from cells expressing a recombinant nucleocapsid protein. The specificity of the interaction was demonstrated by competition experiments with nonlabeled Ps containing RNAs, tRNA, and total cytoplasmic RNA. The results indicated that no virus specific modification of the N-protein or the presence of other viral proteins are required for this *in vitro* interaction. The assays described in this report provide us with a powerful tool for studying encapsidation (initiation) in more detail. © 1997

Academic Press

## INTRODUCTION

The murine coronavirus mouse hepatitis virus (MHV) is an enveloped virus containing a positive stranded RNA genome of about 31 kb (Holmes, 1991; Spaan *et al.*, 1988). The virion envelope is composed of a lipid bilayer derived from an internal compartment of the host cell and three or four virus-encoded structural membrane proteins (Luytjes, 1995): the spike protein (S), the membrane protein (M), the small membrane protein (E), and the optional hemagglutinin-esterase protein (HE). The viral envelope surrounds a nucleocapsid with helical symmetry composed of the genomic RNA and multiple copies of the nucleocapsid protein (N). Evidence for the presence of a fifth structural envelope protein translated from an internal open reading frame (ORF) within the N gene has been published recently (Fischer *et al.*, 1997).

In infected cells MHV produces a 3' coterminal nested set of subgenomic mRNAs (sgRNAs) which possess an identical 5' leader sequence derived from the 5' end of the genome (Lai *et al.*, 1984; Spaan *et al.*, 1983, 1988). Only genomic length RNA is packaged into virus particles; however, trace amounts of sg RNAs are sometimes detected in purified virus (Makino *et al.*, 1988). Earlier studies (Fosmire *et al.*, 1992; Most *et al.*, 1991) have mapped a region in the 3' end of ORF1b that is essential for encapsidation of defective genomes. Within this re-

gion a domain (from here on called Ps) of 69 nt could be identified that is probably required for the encapsidation of defective genomes (Fosmire *et al.*, 1992). This signal is present in genomic RNA, but not in sgRNAs and it is likely that it has also a similar function in the encapsidation of genomic RNA. Recently, it was demonstrated that the encapsidation of a heterologous RNA by MHV was fully dependent on the presence of this Ps (Woo *et al.*, 1997). Furthermore, it was shown by Bos *et al.* (1997) that transferring the Ps to a sgRNA resulted in the specific encapsidation of this sgRNA, though with reduced efficiency.

The nucleocapsid protein of MHV is a basic phosphoprotein of 454 amino acids and has an apparent molecular weight of approximately 55 kDa (Armstrong *et al.*, 1983; Parker and Masters, 1990; Laude and Masters, 1995). It is phosphorylated exclusively on serine residues (Stohlman and Lai, 1979). The N protein contains 41 of these potential phosphorylation sites, but the exact number and location of phosphoserines have not been identified yet. The basic amino acids are not clustered in strings, but local densities of positive charge can be found, particularly in two regions in the middle of the N protein (Laude and Masters, 1995). In contrast, the C-terminus is quite acidic. The MHV N protein does not contain known RNA binding motifs, like the arginine-rich motif (ARM) or zinc fingers (Draper, 1995; Holmes and Behnke, 1981; Burd and Dreyfuss, 1994).

Interaction of the MHV nucleocapsid protein with the

<sup>1</sup>To whom correspondence and reprint requests should be addressed. Fax: (31)-71-5266761. E-mail: azruviro@virology.azl.nl.

leader RNA has been reported although there is some discrepancy about the specificity of this interaction (Stohman *et al.*, 1988; Bredenbeek, 1990). A leader-RNA binding domain in the N protein was mapped and comprises the two basic regions mentioned above (Nelson and Stohman, 1993; Masters, 1992). Furthermore, specific interaction of the coronavirus infectious bronchitis virus (IBV) nucleocapsid protein with the 3' terminus of the genome has recently been reported (Zhou *et al.*, 1997).

The 69-nt Ps is able to form a stable secondary structure and the integrity of this structure is essential for the encapsidation of defective genomes (Fosmire *et al.*, 1992). It has been postulated (Fosmire *et al.*, 1992) that the Ps functions as an encapsidation initiation site, probably by interacting specifically with the N protein. Initiation of encapsidation by packaging signal/(nucleo)capsid protein interactions has been observed for several other RNA viruses, including alphaviruses, retroviruses, and *Escherichia coli* bacteriophages. (Owen and Kuhn, 1996; Berkowitz *et al.*, 1995; Zhang and Barklis, 1995; Schlesinger *et al.*, 1994; Dupraz and Spahr, 1992; Witherell *et al.*, 1991; Aldovini and Young, 1990; Weis *et al.*, 1989). However, a specific interaction of the MHV N protein with the Ps has not been demonstrated yet.

In this report we have used gel retardation and UV cross-linking assays to study the *in vitro* interaction of MHV-A59 nucleocapsid protein and a small RNA containing the Ps domain. We observed specific interaction between *in vitro* transcripts containing the Ps and N protein isolated from infected cells, but also with N protein extracted from purified viruses. Furthermore, we were able to identify a similar interaction with recombinant nucleocapsid protein expressed in the vaccinia T7 expression system. These experiments underline the possibility of studying the encapsidation of MHV-A59 RNA at a molecular basis and allow us to map important domains in both the nucleocapsid protein as well as the RNA packaging signal.

## MATERIALS AND METHODS

### Cells and viruses

Mouse L cells were grown in Dulbecco's modified Eagle's medium (DMEM; Gibco) supplemented with 8% fetal calf serum. MHV-A59 stocks were grown as described (Spaan *et al.*, 1981). Vaccinia virus vTF7.3 (kindly provided by Dr. B. Moss) stocks were grown on RK13 cells.

### Recombinant DNA techniques

Standard recombinant DNA procedures were used (Sambrook *et al.*, 1989). Restriction enzymes, T4 DNA ligase, and T7 RNA polymerase were obtained from Gibco BRL. The T7 sequencing kit of Pharmacia and [ $\alpha$ - $^{32}$ P]dATP of NEN-Dupont were used for DNA sequence

analysis. All enzyme incubations and biochemical reactions were performed according to the instructions of the manufacturers.

### Construction of plasmids

(i) *pPs290*. A 204-nt fragment containing Ps was obtained by polymerase chain reaction (PCR) using pMIDI-C as a template (Most *et al.*, 1991) and oligonucleotide primers C060 and C061 (Table 1). To obtain pPs290 this fragment was cloned in pCRII using the TA cloning kit (Invitrogen) according to the instructions of the manufacturer.

(ii) *pEMCV-N*. A *Nco*I restriction site was created at the position of the AUG start codon of the N gene by PCR mutagenesis using oligonucleotide primers C261 and C224 (Table 1). The PCR fragment was digested with *Nco*I and *Apa*I and fused to the remaining 3' sequences of the N gene. A consequence of this procedure was that the second amino acid of the N protein was changed from a Ser to an Ala. The reconstituted N gene was then exchanged with the *Nco*I–*Bam*HI fragment of pL1a (Snijder *et al.*, 1996) and the sequence of the *Nco*I–*Apa*I fragment was confirmed by sequence analysis. The final expression vector, pEMCV-N, contained a T7 promoter and EMCV-NTR, followed by the entire N gene and a T7 terminator sequence.

### Preparation of riboprobe

In order to serve as template DNA, pPs290 was linearized with *Bam*HI, extracted with phenol/chloroform, and precipitated with ethanol. Alternatively, templates for the production of Ps180 and Ps $\Delta$ HP RNA were produced by PCR using a 5' oligonucleotide containing the T7 promoter sequence in addition to MHV specific sequences (Table 1). Radiolabeled RNA was synthesized by T7 transcription for 1.5 h at 37°. Reactions contained 1  $\mu$ g of linearized plasmid DNA, 1 mM (each) ATP, CTP, and GTP, 50  $\mu$ M UTP, 10  $\mu$ Ci of [ $\alpha$ - $^{32}$ P]UTP (3000 Ci/mmol), and 25 units of T7 polymerase in a final volume of 25  $\mu$ l transcription buffer (Gibco BRL). The reaction products were extracted with phenol/chloroform, purified on a Sephadex G50 column and precipitated by adding 1/10 volume of 5 M NH<sub>4</sub>Ac (pH 5.2) and 2 vol of ethanol. The amount of incorporated label was determined by TCA precipitation.

### Preparation of protein lysates

(i) *MHV-infected and mock-infected cell lysates*. Mouse L cells were grown to 90% confluency in 20-cm-diameter petri dishes (approx.  $3.8 \times 10^7$  cells per dish) and infected with MHV-A59 at a m.o.i. of 10. Cells were harvested 8 h after infection, washed twice with phosphate buffered saline (PBS), and resuspended in 50  $\mu$ l/dish buffer C (20 mM HEPES (pH 7.9), 420 mM NaCl, 1.5 mM MgCl<sub>2</sub>, 0.2 mM EDTA, 25% glycerol, 0.5 mM

TABLE 1  
Oligonucleotide Sequences and Purposes

Primer	Sequence 5' → 3'	Purpose
C060	<i>GTCCCAAGCTTmGAAAGTTGGAGATTC</i>	5' PCR pPs290
C061	<i>TCCGACGCGTAGAGCTTCATTACC</i>	3' PCR pPs290
		3' PCR Ps180 template
C258	<i>TAATACGACTCACTATAGAAAAGTTGGAGATTC</i>	5' PCR Ps180 template
		5' PCR Ps $\Delta$ HP template
C268	<i>TAGAGCTTCGGCTCGGTTGAAGGC</i>	3' PCR Ps $\Delta$ HP template
C261	<i>ATAGCCATGGCTTTTGTTCTGGGC</i>	5' Oligonucleotide for introduction of a <i>Nco</i> I restriction site at the ATG start codon of the nucleocapsid gene
C224	<i>TGTAGGATCCACTGCACCACCATCCTTCTGG</i>	3' Oligonucleotide for introduction of a <i>Nco</i> I restriction site at the ATG start codon of the nucleocapsid gene

Note. Non-MHV sequences are indicated in italics.

phenylmethylsulfonyl fluoride, 0.5 mM dithiothreitol (DTT) (Dignam *et al.*, 1983). Subsequently, the cells were disrupted by freezing ( $-80^{\circ}$ ) and thawing ( $37^{\circ}$ ) once or by 15 strokes of a Dounce homogenizer. Cellular debris and nuclei were removed by centrifugation for 30 min at 13,000 rpm at  $4^{\circ}$ . The supernatant was aliquoted and stored at  $-80^{\circ}$ . The protein concentration was determined using the Bicinchoninic Acid Protein Assay Kit (Sigma).

(ii) *Protein lysates from purified viruses.* Virus was purified as described before (Luytjes *et al.*, 1997). Briefly, viruses harvested from  $8 \times 10^7$  cells were precipitated with polyethylene glycol and loaded on top of a 20 to 50% linear sucrose gradient. The gradient was centrifuged for 16 h at 16,000 rpm at  $4^{\circ}$  in a SW40Ti rotor. Subsequently the gradient was fractionated into 16 fractions. All fractions were assayed for viral proteins by Western blot using the rabbit polyclonal MHV-A59 antiserum k134. The two fractions corresponding to the virus peak and two bottom fractions (control) were combined, and their volumes were adjusted to 5 ml with TESV (20 mM Tris (pH 7.4), 1 mM EDTA, 100 mM NaCl). Virus was pelleted by centrifugation in a SW55Ti rotor for 3 h at 35,000 rpm at  $4^{\circ}$ . The resulting virus pellet was lysed in 100  $\mu$ l buffer C supplemented with 0.5% NP-40.

(iii) *Recombinant N protein lysates.* Vaccinia virus infections and DNA transfections were performed as described previously (Bos *et al.*, 1996). Briefly, RK13 cells were grown to subconfluency in 5-cm-diameter petri dishes ( $4 \times 10^6$  cells per dish) and infected with the T7 RNA polymerase expressing vaccinia virus recombinant (vTF7.3) at a m.o.i. of 5. At 1 h postinfection the cells were transfected with 20  $\mu$ l lipofectin (Gibco BRL) containing 5  $\mu$ g of pEMCV-N. After an incubation of 16 h protein lysates were made as described above.

### Gel mobility shift assays

RNA binding reactions contained 10 ng of radiolabeled riboprobe and 4  $\mu$ g of protein lysate in a final volume of

10  $\mu$ l binding buffer (5 mM HEPES (pH 7.9), 50 mM KAc, 2.4 mM MgAc<sub>2</sub>, 0.1 mM EDTA, 0.01 mM DTT, 1 mM ATP, 0.4 mM GTP). Where necessary specific or nonspecific competitor RNA was added as indicated in the figure legends. In supershift experiments, 1  $\mu$ l of the N-specific monoclonal antibody 5B188.2 (Talbot and Buchmeier, 1985) or  $\beta$ -galactosidase monoclonal antibody (Boehringer Mannheim) and 18 units of RNAGuard (Pharmacia) were added. The mixtures were incubated at room temperature for 20 min, after which 5  $\mu$ l of 50% glycerol was added to each reaction. The mixtures were then separated by electrophoresis on a 5% polyacrylamide/10% glycerol gel (mono:bis = 37.5:1) in 0.5 $\times$  TBE (45 mM Tris-Cl (pH 7.5)), 45 mM boric acid, 1 mM EDTA) for 6 h at 5 mA (fixed). Subsequently, the gel was dried and exposed to X-ray film with an intensifying screen at  $-80^{\circ}$ .

### UV cross-linking

RNA binding reactions were performed as described above. Subsequently the samples were irradiated at a 2-cm distance with 1.8 J/cm<sup>2</sup> of 254-nm UV light in a Stratlinker 1800 (Stratagene). The complexes were then incubated with a mixture of 500 ng RNase A (Pharmacia) and 2.5 units RNase T1 (Gibco BRL) for 20 min at  $37^{\circ}$ . The complexes were analyzed by sodium dodecyl sulfate-polyacrylamide gel electrophoresis on 15% gels.

Alternatively, cross-linked and RNase treated samples were immunoprecipitated prior to electrophoresis as described earlier (Bos *et al.*, 1996) with monoclonal antibody 5B188.2 (Talbot and Buchmeier, 1985) or rabbit polyclonal MHV-A59 antiserum k134.

## RESULTS

### Ps290 RNA binds specifically to proteins from MHV-infected and mock-infected cells

In the studies described here we have analyzed the interaction between the MHV-A59 N protein and RNAs containing the 69-nt Ps signal. In order to identify this

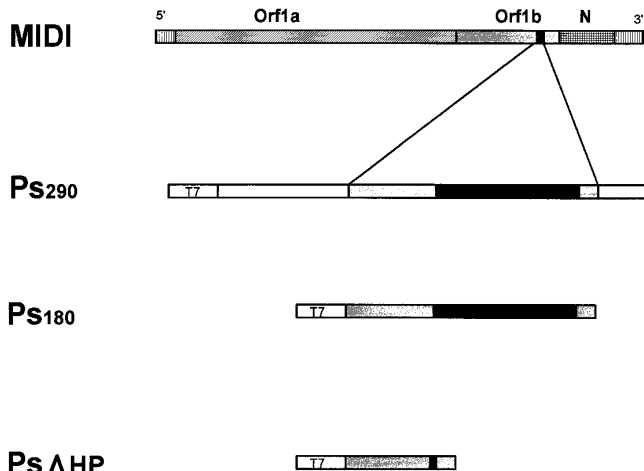


FIG. 1. Schematic representation of RNA probes. The black box indicates the MHV-A59 packaging signal; shaded boxes indicate MHV-specific sequences; open boxes indicate non-MHV sequences.

interaction we have first used gel mobility shift assays using protein lysates from both MHV-infected and mock-infected cells and an *in vitro* transcript containing the Ps (Fig. 1). From pilot experiments using 10 ng of labeled RNA we determined that approximately 4  $\mu$ g of protein lysate was required to observe a distinct retarded band (data not shown). We therefore used these amounts as standard in all binding experiments.

An interaction between Ps290 RNA and proteins from infected cells (I-lysate), as well as from mock-infected cells (MI-lysate) was readily observed (Fig. 2, lanes 2 and 9). However, the complex formed between Ps290 RNA and proteins from the MI-lysate migrated slightly slower in the gel and appeared to be more diffuse, indicating that there are some differences in binding activity between I- and MI-lysates.

In order to determine the specificity of the interaction, competition experiments were performed. Competition of the interaction between Ps290 RNA and proteins from the I-lysate with a 10-fold molar excess of nonlabeled Ps290 RNA resulted already in a decrease of intensity of the retarded band (Fig. 2, lane 5). At a level of 30-fold molar excess of nonlabeled Ps290 RNA the retarded band was no longer visible and all of the labeled RNA migrated at the position of the unbound RNA probe (Fig. 2, lane 7). Competition with a 100-fold molar excess of yeast tRNA did not affect the intensity or the mobility of the retarded band, indicating that the observed interaction between Ps290 RNA and proteins from the I-lysate is specific for the Ps290 RNA (Fig. 2, lane 8). Competition of the interaction between Ps290 RNA and proteins from the MI-lysate with non-labeled Ps290 RNA or yeast tRNA showed a similar result. A 30-fold molar excess of unlabeled Ps290 RNA competed entirely for protein binding (Fig. 2, lane 14), whereas a 100-fold molar excess of yeast tRNA had no effect on the interaction (Fig. 2, lane

15). These observations indicate that there is a specific interaction between Ps290 RNA and proteins from MHV-infected cells as well as with proteins from mock-infected cells.

### The MHV-A59 nucleocapsid protein interacts specifically with Ps290 RNA

To investigate whether the N protein is part of the protein-Ps290 RNA complex, a supershift assay using a N-specific antibody was performed. If the N protein is indeed part of the complex, binding to N of a N-specific antibody should result in the formation of a large complex composed of Ps290 RNA, N protein, and N-specific antibody. This complex is expected to migrate slower in the gel as compared to the protein-Ps290 RNA complex and should be visible as a so-called supershift. The monoclonal N-specific antibody 5B188.2 (Talbot and Buchmeier, 1985) was used to analyze the protein-Ps290 RNA complex and the monoclonal  $\beta$ -galactosidase-specific antibody was used as a control. When N-specific antibody 5B188.2 was added to the complex formed between Ps290 RNA and proteins from the I-lysate, a second complex, migrating slightly slower than the protein-Ps290 RNA complex was readily observed (Fig. 3, lane 5). In contrast, addition of 5B188.2 to the complex formed between Ps290 RNA and proteins from the MI-lysate did not result in a supershift (Fig. 3, lane 13). This demonstrates the presence of the MHV-A59 N protein in the complex formed between Ps290 RNA and proteins from the I-lysate.

The  $\beta$ -galactosidase-specific antibody was not able to shift the complex formed between Ps290 RNA and proteins from the I-lysate or from the MI-lysate (Fig. 3, lanes 11 and 19). Furthermore, incubation of Ps290 RNA and antibody 5B188.2 or  $\beta$ -galactosidase-specific antibody without protein lysate, did not result in the formation of

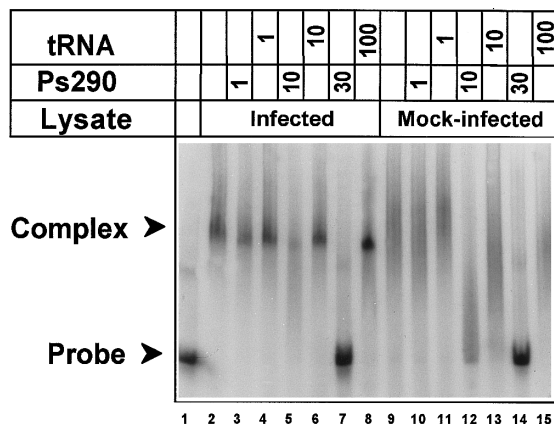


FIG. 2. Gel retardation assay performed with Ps290 probe and protein lysates from infected- or mock-infected cells. Competition was performed using a 1- to 30-fold molar excess of unlabeled Ps290 RNA or a 1- to 100-fold molar excess of yeast tRNA. The positions of the unbound RNA (probe) and complexed RNA (complex) are indicated.

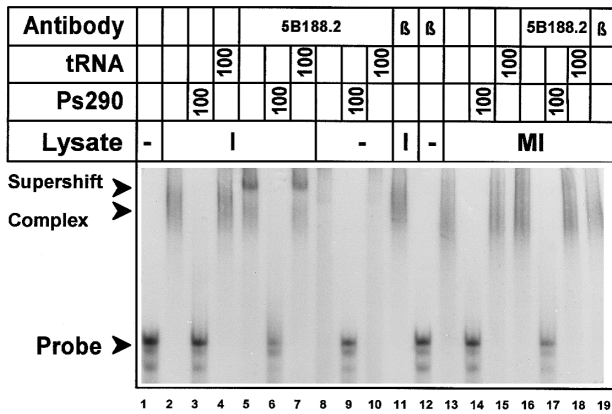


FIG. 3. Gel supershift assay performed with Ps290 probe and protein lysates from infected (I) or mock-infected (MI) cells. The complex was supershifted with either N-specific antibody (5B188.2) or nonspecific  $\beta$ -galactosidase antibody ( $\beta$ ). Competition was performed using a 100-fold molar excess of yeast tRNA. The positions of the unbound RNA (probe), complexed RNA (complex), and supershift are indicated.

RNA–protein complexes (Fig. 3, lanes 8–10 and 12), clearly indicating that the observed supershift was not the result of an interaction between the RNA probe and the N-specific antibody.

Addition of a 100-fold molar excess of nonlabeled Ps290 competitor RNA resulted in the complete inhibition of protein binding to the RNA probe (Fig. 3, lane 6). In contrast, a 100-fold molar excess of tRNA did not affect the formation of RNA–protein and RNA–protein–antibody complexes (Fig. 3, lane 7), which demonstrates the specificity of the interaction between the N protein and Ps290 RNA.

#### UV cross-linking demonstrates specific nucleocapsid protein Ps180-RNA interaction

Another assay for studying the interaction between the N protein and Ps containing RNAs is UV cross-linking. To exclude the possibility that the non-MHV-specific sequences present in Ps290 RNA are involved in the interaction between the nucleocapsid-protein and Ps290 RNA, an RNA probe (Ps180) containing only MHV-specific sequences was constructed. Furthermore, in order to investigate whether the 69-nt hairpin of Ps180 (and Ps290) RNA is responsible for specific nucleocapsid protein binding, Ps $\Delta$ HP RNA was constructed. This RNA is identical to Ps180 RNA except that the largest part of the 69-nt Ps hairpin has been removed. The U contents of Ps180 and Ps $\Delta$ HP are similar (approx. 25%).

Pilot experiments were performed to estimate the optimal UV dose. From these experiments it was determined that an UV dose of 1.8 J/cm<sup>2</sup> gave the most distinct bands with the least background (data not shown).

In all experiments performed with Ps180 RNA or Ps $\Delta$ HP RNA, 5  $\mu$ g of total cytoplasmic RNA extracted from uninfected cells was added as nonspecific competi-

tor RNA. Cross-linked and RNase treated samples were immunoprecipitated with the monoclonal N-specific antibody 5B188.2 or the rabbit polyclonal MHV-A59 antiserum k134 as indicated in the figure legends.

An interaction between the N protein and Ps180 RNA was readily observed (Fig. 4, lane 1), but no interaction was observed between the N-protein and Ps $\Delta$ HP RNA (Fig. 4, lane 2). Complexes formed between proteins from the MI-lysate and Ps180 RNA or Ps $\Delta$ HP RNA could not be immunoprecipitated with the N-specific antibody (Fig. 4, lanes 3 and 4). When the Ps180 and Ps $\Delta$ HP RNAs were used in a competitive gelretardation experiment with radiolabeled Ps290 and the I-lysate, complete competition was observed with the Ps180 RNA, whereas no competition was observed with the Ps $\Delta$ HP RNA (data not shown). These results show that the interaction between the N-protein and Ps180 RNA can also be demonstrated by using an UV cross-linking assay followed by immunoprecipitation and that this interaction is dependent on the presence of the 69-nt Ps hairpin.

To determine the specificity of the nucleocapsid protein–Ps180 RNA interaction in UV cross-linking assays, competition experiments were performed. Addition of a 100-fold molar excess of nonlabeled Ps180 RNA resulted in the complete inhibition of N protein binding (Fig. 5, lane 2), whereas, a 100-fold molar excess of tRNA had no effect on the interaction between the N protein and Ps180 RNA (Fig. 5, lane 3). This clearly demonstrates the specificity of the interaction between the N protein and Ps180 RNA.

#### Nucleocapsid protein from purified viruses and recombinant expressed nucleocapsid protein interact specifically with Ps180 RNA

During RNA encapsidation or particle formation, the N protein might undergo structural changes or other modifications. It would therefore be interesting to see if the N protein incorporated in virus particles is still able to inter-

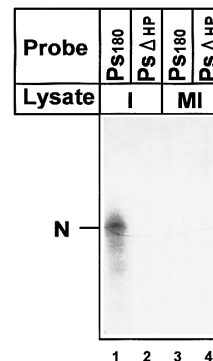


FIG. 4. UV cross-linking experiment performed with Ps180 or Ps $\Delta$ HP probe in the presence of 5  $\mu$ g of cytoplasmic RNA followed by immunoprecipitation with 5B188.2. Infected cell lysates (I) or mock-infected cell lysates (MI) were used. The position of the N-specific band is indicated.

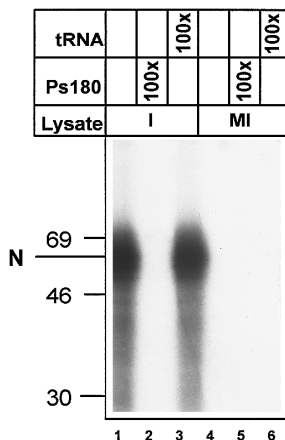


FIG. 5. UV cross-linking experiment performed with Ps180 probe and protein lysates from infected (I) or mock-infected (MI) cells. Complexes were immunoprecipitated with N-specific monoclonal antibody 5B188.2. Competition was performed with unlabeled Ps180 RNA or yeast tRNA as indicated above the lanes. The position of the N-protein specific band is indicated.

act specifically with Ps180. In order to address this question, virus particles were purified on a sucrose gradient. Lysates were prepared from the virus peak fractions (p-lysate) and from the gradient bottom fractions (b-lysate; negative control). UV cross-linking was performed using both lysates, radiolabeled Ps180 RNA, and competitor RNA (5  $\mu$ g of total cytoplasmic RNA extracted from uninfected cells; Fig. 6B). A specific interaction was observed between the N-protein from the p-lysate and Ps180 RNA (Fig. 6B, lanes 2 and 4). In contrast, no complex could be immunoprecipitated with N-specific antibodies when the b-lysate was used (Fig. 6B, lanes 1 and 3). This indicates that any structural change of the N protein which might occur during virus assembly does not affect the ability of the N protein to interact with Ps180 RNA.

In MHV-infected cells, the N protein might also undergo virus-specific or virus-dependent posttranslational modifications. These modifications might play a role in the specific interaction with the Ps. Furthermore, it is not yet known if the interaction between the N protein and the Ps involves other viral proteins as well. In order to investigate this, recombinant N protein was expressed by the vTF7.3 expression system. A N protein expression vector (pEMCV-N) was transfected in vTF7.3-infected RK13 cells and protein lysates were made 16 h post-transfection (vTF7pN lysate). As a control protein lysates from mock-transfected but vTF7.3-infected RK13 cells were made (vTF7-lysate). UV cross-linking experiments, followed by immunoprecipitation with N-specific antibody 5B188.2, were performed with both lysates using radiolabeled Ps180 RNA and competitor RNA (5  $\mu$ g of total cytoplasmic RNA extracted from uninfected cells; Fig. 6C). Using the vTF7pN lysate, a clear band was observed migrating at the expected position of the nucleocapsid protein (Fig. 6C, lane 1). This band was not

observed using the vTF7-lysate (Fig. 6C, lane 2). These experiments clearly demonstrate that no virus specific modifications of the N protein or any other viral proteins are required for the specific interaction with Ps180.

## DISCUSSION

### Specific interaction of the MHV nucleocapsid protein with Ps containing RNAs

Initiation of encapsidation by a specific interaction between the (nucleo-) capsid protein and a RNA packaging signal is a common mechanism used by positive stranded RNA viruses. Such an interaction has already been identified and studied *in vitro* in alphaviruses (Owen and Kuhn, 1996; Weis *et al.*, 1989), retroviruses (Zhang and Barklis, 1995; Berkowitz *et al.*, 1995; Dupraz and Spahr, 1992; Aldovini and Young, 1990) but also in *E. coli* bacteriophages like R17 and MS2 (Witherell *et al.*, 1991). In this report we describe the specific *in vitro* interaction of the mouse hepatitis virus A59 N protein with transcripts containing the RNA packaging signal of MHV. This interaction was studied by gel retardation and UV cross-linking assays using an RNA probe containing the 69-nt Ps and the N protein from MHV-A59 infected cell lysates. A similar interaction was identified between the N protein from purified virus and recombinant N-protein expressed by the vTF7 expression system.

In addition to the N-Ps RNA complex we also observed that cellular proteins bind to Ps containing RNAs. The nature of these cellular proteins and the significance of this interaction, however, remains unclear.

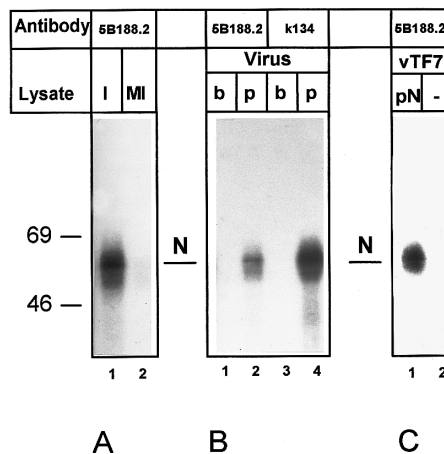


FIG. 6. UV cross-linking experiment performed with Ps180 probe in the presence of 5  $\mu$ g of cytoplasmic RNA. Protein lysates from (A) infected (I) and mock-infected (MI) cells, protein lysates from (B) gradient purified virions, and protein lysates from (C) vTF7 infected and pEMCV-N (pN) transfected cells were used. b denotes the bottom-fraction lysate and p denotes the peak-fraction lysate. Immunoprecipitation with 5B188.2 and k134 were performed as indicated above the lanes. The position of the N-protein-specific band is indicated.

## The nature of the nucleocapsid protein–Ps RNA interaction

The N-protein of MHV does not possess any well known RNA binding domains, such as the ARM (Lazinski *et al.*, 1989; Talbot and Buchmeier, 1985) or zinc fingers (Draper, 1995). It interacts, although, specifically with leader-RNA (Stohlman *et al.*, 1988; Baric *et al.*, 1988) and an RNA binding domain has been identified (Nelson and Stohlman, 1993). This domain comprises the two major hydrophobic basic regions in the middle of the protein. Since this central part of the N protein contains a high degree of basic amino acids, it is possible that the Ps recognition domain might also be positioned somewhere within this part of the N protein.

In infected cells the N protein of MHV is very rapidly phosphorylated on serine residues (Stohlman and Lai, 1979) and part of it concomitantly becomes associated with a cell membrane fraction (Stohlman *et al.*, 1983; Anderson and Wong, 1993). It is still unknown if phosphorylation is carried out by a host cell or viral encoded protein kinase and its (biological) role remains unclear. It has been suggested that it might govern the tightness of the interaction between N and RNA (Laude and Masters, 1995). It will be interesting to compare the phosphorylation of the N protein from infected cells and the recombinant N protein and to investigate the possible role of phosphorylation in RNA binding. Phosphorylation and likewise dephosphorylation could also induce a major conformational change of the N protein. It has been suggested that dephosphorylation of the nucleocapsid after virus entry is involved in uncoating of the viral RNA (Mahondas and Dales, 1991).

In general the recognition of an RNA signal by a protein involves secondary structure elements in addition to the primary sequence of the RNA signal (Draper, 1995). There is accumulating evidence for an induced-fit mechanism in RNA–protein interactions affecting both the RNA and the protein (Beck and Nassal, 1997; Allain *et al.*, 1996). Sufficient flexibility in the RNA molecule could be a major determinant in protein binding. From that perspective, the recognition of the Ps by the N protein could be highly dependent on the secondary structure of the Ps domain. When a short RNA probe consisting of only the 69-nt Ps was used in our studies, no gel retardation or UV cross-linking to the N protein was observed (unpublished observations). Computer prediction of the secondary structure of this small 69-nt RNA molecule showed that the secondary structure was entirely different from that of the Ps in the ORF1b context. This suggests that the flanking ORF1b sequences are necessary to force the Ps in its specific structure or that the small RNA probe lacks the flexibility to form the specific structure. Recently, it has been shown that the 69-nt Ps, flanked by non-MHV sequences could confer specific encapsidation to a heterologous RNA in MHV infected

cells (Woo *et al.*, 1997). Although it is not known whether this encapsidation was efficient, it might be possible that the heterologous flanking sequences have increased the flexibility of the RNA molecule, allowing it to adapt the proper structure for encapsidation.

## Significance of the nucleocapsid protein–Ps RNA interaction

Since MHV virions contain only MHV genomic RNA, it is evident that RNA encapsidation is a highly specific process. The location of the encapsidation signal in ORF1b ensures the specific encapsidation of only genomic RNA. It is unclear if the MHV Ps is by itself sufficient for efficient encapsidation. It is known that Rous sarcoma virus has multiple encapsidation sites, which are required to interact for efficient packaging of the genome (Sorge *et al.*, 1983; Pugatsch and Stacey, 1983). Recently, it was shown that a subgenomic RNA of MHV containing the Ps can be encapsidated specifically but the efficiency was much lower as compared to the encapsidation efficiency of a defective interfering RNA (Bos *et al.*, 1997).

Preassembled nucleocapsids have never been observed in coronavirus infected cells, but an electron-dense structure, which may correspond to the nucleocapsid, can be found at the cytoplasmic face of the budding site (Dubois-Dalcq *et al.*, 1982; Holmes, 1991). Nucleocapsid incorporation in budding virions is expected to be mediated by M–N protein interactions. Association of the M protein to the nucleocapsid in NP-40-disrupted virions has been reported (Sturman *et al.*, 1980); however, the same study demonstrated that the M protein was able to bind RNA in the absence of N. It is still unclear if the interaction between M and N is a prerequisite for RNA encapsidation *in vivo*. This interaction could position the N protein in a favorable way to interact with the genomic RNA. This must then be followed by interaction with additional N proteins, forming the helical nucleocapsid. Involvement of other viral proteins in Ps RNA binding, however, was not observed in our *in vitro* studies. Recombinant nucleocapsid protein, expressed in the vTF7 expression system, interacts also specifically with the Ps RNA (Fig. 6C), although the efficiency of this interaction was not determined. A striking feature of coronaviruses is that the nucleocapsid has a helical symmetry (MacNaughton *et al.*, 1978; Holmes and Behnke, 1981), in contrast to the nucleocapsids of all other positive stranded RNA viruses, which are icosahedral or spherical (Murphy *et al.*, 1995). However, electron microscopy studies on the transmissible gastroenteritis coronavirus and MHV (Risco *et al.*, 1996) have revealed recently a spherical core structure inside the virion (internal core) and this structure reacted with M- and N-specific antibodies. A structural model for coronaviruses was proposed, in which a spherical core, composed of a combination of N and M proteins, was present in addition to



a helical nucleocapsid. It will be of interest to study the possible relationship between the morphology of the nucleocapsid or internal core and the mechanism of encapsidation initiation.

It has been shown that, as opposed to alphavirus assembly, nucleocapsid formation and RNA encapsidation are not strictly required for virion formation (Vennema *et al.*, 1996; Bos *et al.*, 1996; Strauss and Strauss, 1994). Coexpression of M and E protein was sufficient for particle formation. However, incorporation of nucleocapsids during the budding process could greatly increase the efficiency of virion formation.

The study of the encapsidation of coronaviruses is greatly hampered by the absence of an infectious clone. The *in vitro* binding assay, described in this report, can greatly enhance our understanding of the encapsidation mechanism. We have shown that recombinant nucleocapsid protein expressed in the vTF7 expression system is able to interact with the Ps in a similar fashion as the nucleocapsid protein produced in infected cells. Mutational analysis of both the nucleocapsid protein and the Ps should provide us with information that allows us to understand the encapsidation mechanism in more detail.

## ACKNOWLEDGMENTS

We thank Willem Luytjes, Evelyne Bos, Guido van Marle, Jessika Dobbe, and Heleen Gerritsma for stimulating discussions. R.M. was supported by Grant 700-31-020 from the Dutch Foundation for Chemical Research (SON).

## REFERENCES

- Aldovini, A., and Young, R. A. (1990). Mutations of RNA and protein sequences involved in human immunodeficiency virus type 1 packaging result in production of noninfectious virus. *J. Virol.* **64**, 1920–1926.
- Allain, F. H.-T., Gubser, C. C., Howe, P. W. A., Nagai, K., Neuhaus, D., and Varani, G. (1996). Specificity of ribonucleoprotein interaction determined by RNA folding during complex formation. *Nature* **380**, 646–650.
- Anderson, R., and Wong, F. (1993). Membrane and phospholipid binding by murine coronaviral nucleocapsid N protein. *Virology* **194**, 224–232.
- Armstrong, J., Smeekens, S., and Rottier, P. J. M. (1983). Sequence of the Nucleocapsid gene from murine coronavirus MHV-A59. *Nucleic Acids Res.* **11**, 883–891.
- Baric, R. S., Nelson, G. W., Fleming, J. O., Deans, R. J., Keck, J. G., Cas-teel, N., and Stohman, S. A. (1988). Interactions between coronavirus nucleocapsid protein and viral RNAs: Implications for viral transcription. *J. Virol.* **62**, 4280–4287.
- Beck, J., and Nassal, M. (1997). Sequence- and structure-specific determinants in the interaction between the RNA encapsidation signal and reverse transcriptase of avian hepatitis B viruses. *J. Virol.* **71**, 4971–4980.
- Berkowitz, R. D., Ohagen, A., Hoglund, S., and Goff, S. P. (1995). Retroviral nucleocapsid domains mediate the specific recognition of genomic viral RNAs by chimeric gag polyproteins during RNA packaging *in vivo*. *J. Virol.* **69**, 6445–6456.
- Bos, E. C. W., Luytjes, W., Meulen van der, H., Koerten, H. K., and Spaan, W. J. M. (1996). The production of recombinant infectious DI-particles of a murine coronavirus in the absence of helper virus. *Virology* **218**, 52–60.
- Bos, E. C. W., Dobbe, J., Luytjes, W., and Spaan, W. J. M. (1997). A sub-genomic mRNA transcript of the coronavirus mouse hepatitis virus strain A59 defective interfering (DI) RNA is packaged when it contains the DI packaging signal. *J. Virol.* **71**, 5684–5687.
- Bredenbeek, P. J. (1990). "Nucleic Acid Domains and Proteins Involved in the Replication of Coronaviruses." Ph.D. Thesis, University of Utrecht, Utrecht, The Netherlands.
- Burd, C. G., and Dreyfuss, G. (1994). Conserved structures and diversity of functions of RNA-binding proteins. *Science* **265**, 615–621.
- Dignam, J. D., Lebowitz, R. M., and Roeder, R. G. (1983). Accurate transcription initiation by RNA polymerase II in a soluble extract from isolated mammalian nuclei. *Nucleic Acids Res.* **11**, 1475–1489.
- Draper, D. E. (1995). Protein-RNA recognition. *Annu. Rev. Biochem.* **64**, 593–620.
- Dubois-Dalcq, M. E., Doller, E. W., Haspel, M. V., and Holmes, K. V. (1982). Cell tropism and expression of mouse hepatitis viruses (MHV) in mouse spinal cord cultures. *Virology* **119**, 317–331.
- Dupraz, P., and Spahr, P. F. (1992). Specificity of Rous sarcoma virus nucleocapsid protein in genomic RNA packaging. *J. Virol.* **66**, 4662–4670.
- Fischer, F., Peng, D., Hingley, S. T., Weiss, S. R., and Masters, P. S. (1997). The internal open reading frame within the nucleocapsid gene of mouse hepatitis virus encodes a structural protein that is not essential for viral replication. *J. Virol.* **71**, 996–1003.
- Fosmire, J. A., Hwang, K., and Makino, S. (1992). Identification and characterization of a coronavirus packaging signal. *J. Virol.* **66**, 3522–3530.
- Holmes, K. V. (1991). In "Fundamental Virology" (B. N. Fields and D. M. Knipe, Eds.), pp. 471–486. Raven Press, New York.
- Holmes, K. V., and Behnke, J. N. (1981). Evolution of a coronavirus during persistent infection *in vitro*. *Adv. Exp. Med. Biol.* **142**, 287–299.
- Lai, M. M. C., Baric, R. S., Brayton, P. R., and Stohman, S. A. (1984). Characterization of leader RNA sequences on the virion and mRNAs of mouse hepatitis virus, a cytoplasmic RNA virus. *Proc. Natl. Acad. Sci. USA* **81**, 3626–3630.
- Laude, H., and Masters, P. S. (1995). In "The Coronaviridae" (S. G. Siddell, Ed.), pp. 141–163. Plenum Press, New York.
- Lazinski, D., Gradzielska, E., and Das, A. (1989). Sequence specific recognition of RNA hairpins by bacteriophage antiterminators requires a conserved arginine-rich motif. *Cell* **59**, 207–215.
- Luytjes, W. (1995). In "The Coronaviridae" (S. G. Siddell, Ed.), pp. 33–54. Plenum, New York.
- Luytjes, W., Gerritsma, H., Bos, E. C. W., and Spaan, W. J. M. (1997). Characterisation of two temperature-sensitive mutants of coronavirus mouse hepatitis virus strain A59 with maturation defects in the spike protein. *J. Virol.* **71**, 949–955.
- MacNaughton, M. R., Davies, H. A., and Nermut, M. V. (1978). Ribonucleoprotein-like structures from coronavirus particles. *J. Gen. Virol.* **39**, 545–549.
- Mahondas, D. V., and Dales, S. (1991). Endosomal association of a protein phosphatase with high dephosphorylation activity against a coronavirus nucleocapsid protein. *FEBS Lett.* **282**, 419–424.
- Makino, S., Shieh, C., Soe, L. H., Baker, S. C., and Lai, M. M. C. (1988). Primary structure and translation of a defective interfering RNA of murine coronavirus. *Virology* **166**, 1–11.
- Masters, P. S. (1992). Localization of an RNA-binding domain in the nucleocapsid protein of the coronavirus mouse hepatitis virus. *Arch. Virol.* **125**, 141–160.
- Most, v. d., R. G., Bredenbeek, P. J., and Spaan, W. J. M. (1991). A domain at the 3' end of the polymerase gene is essential for encapsidation of coronavirus defective interfering RNAs. *J. Virol.* **65**, 3219–3226.
- Murphy, F. A., Fauquet, C. M., Bishop, D. H. L., Ghabrial, S. A., Jarvis, A. W., Martinelli, G. P., Mayo, M. A., and Summers, M. D. (1995). "Virus

- Taxonomy, Classification and Nomenclature of Viruses." Springer-Verlag, New York.
- Nelson, G. W., and Stohman, S. A. (1993). Localization of the RNA-binding domain of mouse hepatitis virus nucleocapsid protein. *J. Gen. Virol.* **74**, 1975–1979.
- Owen, K. E., and Kuhn, R. J. (1996). Identification of a region in the Sindbis virus nucleocapsid protein that is involved in specificity of RNA encapsidation. *J. Virol.* **70**, 2757–2763.
- Parker, M. M., and Masters, P. S. (1990). Sequence comparison of the N genes of five strains of the coronavirus mouse hepatitis virus suggests a three domain structure for the nucleocapsid protein. *Virology* **179**, 463–468.
- Pugatsch, T., and Stacey, D. W. (1983). Identification of a sequence likely to be required for avian retroviral packaging. *Virology* **128**, 505–511.
- Risco, C., Anton, I. M., Enjuanes, L., and Carrascosa, J. L. (1996). The transmissible gastroenteritis coronavirus contains a spherical core shell consisting of M and N proteins. *J. Virol.* **70**, 4773–4777.
- Sambrook, J., Fritsch, E. F., and Maniatis, T. (1989). "Molecular Cloning: A Laboratory Manual," 2nd ed. Cold Spring Harbor Laboratory Press, Cold Spring Harbor, NY.
- Schlesinger, S., Makino, S., and Linial, M. L. (1994). *Cis*-acting genomic elements and *trans*-acting proteins involved in the assembly of RNA viruses. *Semin. Virol.* **5**, 39–49.
- Snijder, E. J., Wassenaar, A. L. M., Dinten, v., L. C., Spaan, W. J. M., and Gorbalenya, A. E. (1996). The arterivirus Nsp4 protease is the prototype of a novel group of chymotrypsin-like enzymes, the 3C-like serine proteases. *J. Biol. Chem.* **271**, 4864–4871.
- Sorge, J., Ricci, W., and Hughes, S. H. (1983). *cis*-Acting RNA packaging locus in the 115-nucleotide direct repeat of Rous sarcoma virus. *J. Virol.* **48**, 667–675.
- Spaan, W. J. M., Rottier, P. J. M., Horzinek, M. C., and Van der Zeijst, B. A. M. (1981). Isolation and identification of virus-specific mRNAs in cells infected with mouse hepatitis virus (MHV-A59). *Virology* **108**, 424–434.
- Spaan, W. J. M., Delius, H., Skinner, M. A., Armstrong, J., Rottier, P. J. M., Smeekens, S., Van der Zeijst, B. A. M., and Siddell, S. G. (1983). Coronavirus mRNA synthesis involves fusion of non-contiguous sequences. *EMBO J.* **2**, 1839–1844.
- Spaan, W. J. M., Cavanagh, D., and Horzinek, M. C. (1988). Coronaviruses: structure and genome expression. *J. Gen. Virol.* **69**, 2939–2952.
- Stohman, S. A., Fleming, J. O., Patton, C. D., and Lai, M. M. C. (1983). Synthesis and subcellular localization of the murine coronavirus nucleocapsid protein. *Virology* **130**, 527–532.
- Stohman, S. A., Baric, R. S., Nelson, G. W., Soe, L. H., Welter, L. M., and Deans, R. J. (1988). Specific interaction between coronavirus leader RNA and nucleocapsid protein. *J. Virol.* **62**, 4288–4295.
- Stohman, S. A., and Lai, M. M. C. (1979). Phosphoproteins of murine hepatitis viruses. *J. Virol.* **32**, 672–675.
- Strauss, J. H., and Strauss, E. G. (1994). The alphaviruses: gene expression, replication, and evolution [published erratum appears in *Microbiol. Rev.*, 1994 Dec, **58**(4), 806]. *Microbiol. Rev.* **58**, 491–562. [Review]
- Sturman, L. S., Holmes, K. V., and Behnke, J. (1980). Isolation of coronavirus envelope glycoproteins and interaction with the viral nucleocapsid. *J. Virol.* **33**, 449–462.
- Talbot, P. J., and Buchmeier, M. J. (1985). Antigenic variation among murine coronaviruses: Evidence for polymorphism on the peplomer glycoprotein, E2. *Virus Res.* **2**, 317–328.
- Vennema, H., Godeke, G.-J., Rossen, J. W. A., Voorhout, W. F., Horzinek, M. C., Opstelten, D.-J. E., and Rottier, P. J. M. (1996). Nucleocapsid-independent assembly of coronavirus-like particles by co-expression of viral envelope protein genes. *EMBO J.* **15**, 2020–2028.
- Weis, B., Nitschko, H., Ghattas, I., and Schlesinger, S. (1989). Evidence for specificity in the encapsidation of Sindbis virus RNAs. *J. Virol.* **63**, 5310–5318.
- Witherell, G. W., Gott, J. M., and Uhlenbeck, O. C. (1991). Specific interaction between RNA phage coat proteins and RNA. *Prog. Nucleic Acid Res. Mol. Biol.* **40**, 185–220.
- Woo, K., Joo, M., Narayanan, K., Kim, K. H., and Makino, S. (1997). Murine coronavirus packaging signal confers packaging to nonviral RNA. *J. Virol.* **71**, 824–827.
- Zhang, Y., and Barklis, E. (1995). Nucleocapsid protein effects on the specificity of retrovirus RNA encapsidation. *J. Virol.* **69**, 5716–5722.
- Zhou, M., Williams, A. K., Chung, S., Wang, L., and Collisson, E. W. (1997). The infectious bronchitis virus nucleocapsid protein binds RNA sequences in the 3' terminus of the genome. *Virology* **217**, 191–199.